TiO_2/MnO_2 composite electrode enabling photoelectric conversion and energy storage as photoelectrochemical capacitor

Hiroyuki Usui[†,‡,*], *Shin Suzuki*[§,‡], *Yasuhiro Domi*[†,‡], *and Hiroki Sakaguchi*[†,‡]

[†] Department of Chemistry and Biotechnology, Graduate School of Engineering, Tottori University, 4-101 Minami, Koyama-cho, Tottori 680-8552, Japan

[§] Course of Chemistry and Biotechnology, Department of Engineering, Graduate School of Sustainability Science, Tottori University, 4-101 Minami, Koyama-cho, Tottori 680-8552, Japan

[‡] Center for Research on Green Sustainable Chemistry, Tottori University, 4-101 Minami, Koyama-cho, Tottori 680-8552, Japan

Corresponding Author: * Tel./Fax: +81-857-31-5634, E-mail: usui@chem.tottori-u.ac.jp

Abstract

We prepared composite electrodes by using rutile TiO_2 particles and γ-MnO_2 particles, and evaluated their photoelectrochemical capacitor properties based on Na^+ adsorption by light irradiation in aqueous electrolytes. By employing different synthesis method for TiO_2 particles, we synthesized TiO_2 particles with various particle sizes and crystallite sizes. An electrode of sol−gel-synthesized TiO_2 showed higher photovoltages compared with an electrode of commercial TiO_2. This probably originates from a larger contact area between electrode surface and electrolyte because of its smaller particle size than commercial TiO_2's size. A further enhancement in photovoltage was attained for an electrode of a hydrothermally-synthesized TiO_2 with good crystallinity. We consider that electron−hole recombination was suppressed because hydrothermal TiO_2 has a lower density of lattice defect trapping the photoexcited carriers. As photoelectrochemical capacitor, a composite electrode consisting of hydrothermal TiO_2 and MnO_2 exhibited a 2.4 times larger discharge capacity compared with that of commercial TiO_2 and MnO_2. This result is attributed to an increased amount of Na^+ adsorption induced by the enhanced photovoltage of TiO_2.

Keywords: Photoelectrochemical capacitor; Composite electrode; Rutile-type TiO_2; γ-phase MnO_2; Hydrothermal synthesis

1. Introduction

For the realization of a low-carbon society, we should utilize solar energy as effectively as possible because it is an inexhaustible energy resource with no carbon emission. Although photovoltaic cell is one of the most attractive device converting renewable energies into electricity, there are disadvantages such as variation in power generation and a low power density of the solar light. The solar irradiance significantly changes depending on weather, time of day, and location, which is the reason of the variation in power generation. To effectively use the energy, we essentially need a help of energy storage devices. The power density is as low as 1.36 kW m^{-2} on the earth surface, requiring a solar panel system with very large area. In general, silicon-based photovoltaic cells can generate a photovoltage up to 600−800 mV. This voltage is, however, much lower than the charge voltages of 3−4 V required for the operation of Li-ion battery and Na-ion battery. Consequently, the batteries do not operate if a single photovoltaic cell is connected with it. On the other hand, electrochemical capacitors are expected to operate even by lower charge voltages because adsorption reactions of Li ions and Na ions on electrodes require much lower activation energies compared with insertion reactions of Li ions and Na ions into electrodes of the batteries.

A photoelectrochemical capacitor is a novel device enabling both photoelectric conversion and energy storage. The two functions are performed by an irradiation to a semiconductor electrode and by ion adsorption on an electrode. The photoelectrochemical capacitor is expected to be applied the next-generation portable display devices like electronic paper operating by a low power consumption. If this device is realized, such portable devices can be used anywhere on the earth, isolate island, mountain area, deep jungle, and desert.

Several types of photoelectrochemical capacitors have been recently developed by various researcher groups [1-6]. Miyasaka *et al.* have newly developed a three-electrode-type photoelectrochemical capacitor in which a dye-sensitized mesoporous TiO_2 and an activated carbon perform photoelectric conversion and energy storage, respectively [1]. Takahashi and Tatsuma have reported a photoelectrochemical capacitor consisted of a TiO_2 electrode for photoelectric conversion and a WO_3 electrode for energy storage [2]. Joudkazytė *et al.* have developed one using two electrodes of a TiO_2 electrode and a RuO_2 electrode [3]. Chen *et al.* have

prepared a unique wire-shaped device based on carbon fibers wrapped around a TiO_2 nanowire [4]. Skunik-Nuckowska *et al.* [5] and Liu *et al.* [6] have reported integrated systems of photoelectrochemical capacitors. We should note that photoelectric conversion electrode and energy storage electrode are separated in case of these systems [1-6]. Compared to this, the authors consider that the separated electrodes are unfavorable for saving space and weight of device, and that these two functions should be combined into single electrode. Therefore, we are suggesting new TiO_2-based electrodes combining the two functions of photoelectric conversion and energy storage [7,8]. This has a profound significance from the perspective of device configuration.

The authors have previously discovered that a nanostructured TiO_2 film can function as a photoelectrochemical capacitor electrode [7]. The typical mechanism can be explained as shown in Fig. 1 [8]. When a TiO_2 electrode is immersed in an electrolyte such as Na_2SO_4 or $LiClO_4$ aqueous solution, a space charge layer is formed on the TiO_2 surface. (i) An irradiation to the electrode causes photo-excitation to generate electron–hole pairs. (ii) Holes move toward the surface, and are consumed by the oxidation of electrolytes such as OH^- and SO_4^{2-}. Although this oxidation process is irreversible in the current system, we would develop a reversible redox process based on I_3^-/I^- couple like a dye-sensitized solar cell in the future. (iii) On the other hand, electrons move inside TiO_2 because of the electric field of the space charge layer. An electron accumulation lowers the potential of the TiO_2 electrode to attract Na ions (or Li ions) from the electrolyte to the

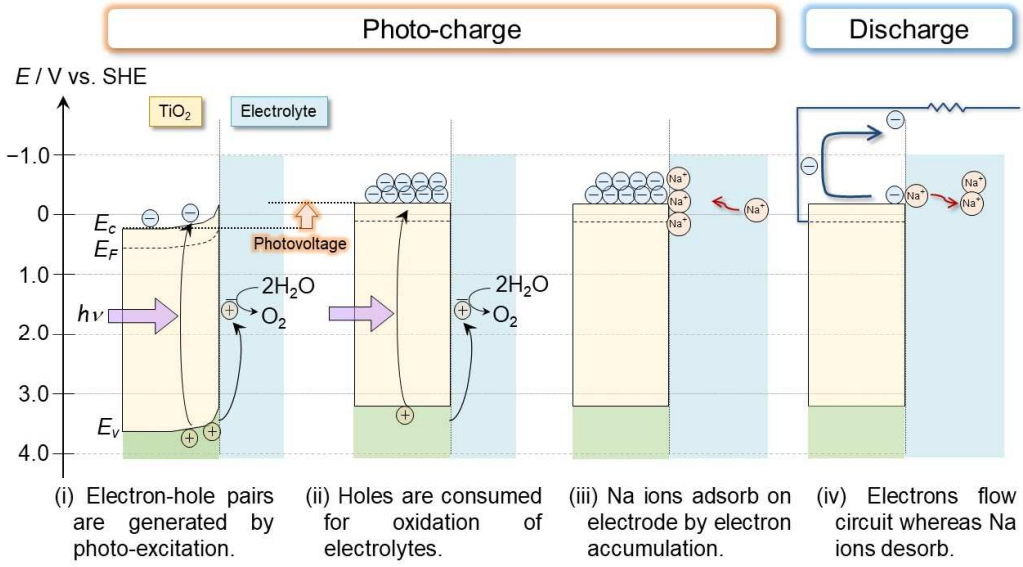

Figure 1. Photo-charge and discharge mechanisms of TiO_2 electrode for photoelectrochemical capacitor.

electrode surface. Na ions are stored at an electric double layer and at the top surface of TiO_2. (iv) If the TiO_2 electrode is connected to a counter electrode by means of an external circuit, the electrons flow through the circuit whereas Na ions desorb and return to the electrolyte. On the basis of this mechanism, photo-charge and discharge were performed. However, the electrode of TiO_2 alone shows a poor discharge capacity owing to the smaller amount of Na-ion adsorption [8].

To overcome this problem, the authors proposed composite electrodes comprised of TiO_2 and Na-storage metal oxides such as $Li_4Ti_5O_{12}$, RuO_2, and MnO_2 [8]. Among them, we have particularly focused MnO_2 because there are MnO_2 polymorphs with various tunnels in their crystal structures which are very suitable for Na-ion storage electrode materials of electrochemical supercapacitor. In fact, the TiO_2/MnO_2 composite electrode exhibited an improved photoelectrochemical performance because MnO_2 has a more preferable crystal structure for Na-adsorption compared with other oxides [8]. For further improvement, the optimization is required not only for MnO_2 but also for TiO_2 in the composite electrode. If the low photovoltage of TiO_2 can be improved, the larger amount of electrons are transferred to MnO_2 to promote the larger amount of Na-adsorption. The efficient electron transfer can be realized by suppressing a recombination of electron−hole pairs in TiO_2. Therefore, we should focus the particle size and crystallinity of TiO_2 as parameters affecting the recombination suppression. In this study, we synthesized some TiO_2 with different particle size and crystallinity, and investigated the photoelectrochemical capacitor properties for composite electrodes prepared using the TiO_2 and MnO_2.

2. Experimental

2.1. TiO_2 synthesis by hydrothermal method

Titanium tetraisopropoxide $Ti[OCH(CH_3)_2]_4$ (95%, Wako Pure Chemical Industries) and isopropanol (99.5%, Sigma-Aldrich) were used as the precursor of titanium dioxide particles and as the solvent to dilute titanium isopropoxide, respectively. A mixture of 5.0 mL of $Ti[OCH(CH_3)_2]_4$ and 5.0 mL of isopropanol was poured into a 50 mL aqueous solution of glycolic acid $HOCH_2CO_2H$ (99.0%, Sigma-Aldrich) with a concentration of 1.6 mol L^{-1}. The glycolic acid

has a function to induce the formation of the rutile polymorph of titanium dioxide. The mixed solution was stirred with 500 rpm at 80 ºC for 1.5 hours. The solution was sealed in a 50 mL Teflon-lined stainless steel autoclave (HU-50, SAN-AI Kagaku) and heated to 200 °C for reaction times of 12 hours, and then was slowly cooled to room temperature. The precipitation was collected by a centrifugal separation for the resulting solution, and was dried at 90 ºC for 12 hours after washing with deionized water and ethanol for three times. Finally, a thermal treatment was performed at 400 ºC in air for 4 hours to remove adsorbed water.

2.2. TiO_2 synthesis by sol−gel method

An 8 mL of hydrochloric acid (HCl, Wako Pure Chemical Industries, 35–37% assay) was diluted in an 112 mL of deionized water. A 4 mL of $Ti[OCH(CH_3)_2]_4$ was poured into the diluted HCl solution with pH of 0.3. The mixed solution was stirred with 500 rpm at 55 ºC for 5 minutes. The detailed procedures were described in the previous paper [9]. The resulting colloidal suspensions was centrifuged and washed with deionized water and ethanol for three times. The washed precipitate was dried under vacuum at 85 ºC for 10 hours, then heated at 400 ºC in air for 10 hours.

2.3. Commercially available TiO_2

A powder of rutile-type titanium dioxide (99.9%, Wako Pure Chemical Industries) was purchased, and was used as received. In general, commercial TiO_2 is industrially prepared by a sulfuric acid method. As a preliminary experiment, we evaluated a photoelectrochemical property of anatase-type TiO_2, and confirmed that the photovoltage of anatase TiO_2 electrode is inferior to that of rutile TiO_2 electrode. In this study, we focus rutile TiO_2 as the photovoltaic electrode material.

2.4. MnO_2 synthesis by hydrothermal method

A 0.48 g of manganese sulfate monohydrate $MnSO_4 \cdot H_2O$ (99%, Sigma-Aldrich) and a 0.54 g of potassium peroxydisulfate (99.0%, Sigma-Aldrich) were mixed in a 40 mL of deionized water. The mixed solution was stirred at room temperature for 10 minutes. The solution was sealed in the Teflon-lined stainless steel autoclave and heated to 200 °C for reaction times of 30 minutes. The reacted solution was quenched by an ice-water to obtain a single phase sample of γ-MnO_2. The

supernatant of the quenched solution was removed by decantation. The precipitate was collected by a centrifugation, and was washed with deionized water and ethanol for three times. The resulting precipitate was dried under vacuum at 60 °C for 8 hours to obtain a brown-colored powder. The powder was confirmed to have a crystal structure of γ-MnO_2 and crystallite size of 8.7 nm (Fig. S1).

2.5. Characterizations

The crystal information of TiO_2 and MnO_2 was acquired by X-ray diffraction (XRD) using an X-ray diffractometer (Ultima IV, Rigaku) with CuKα radiation (λ = 0.154178 nm). The crystallite sizes of the TiO_2 powders were estimated by using the Scherrer equation and full width at half maximums of diffraction peaks. The morphologies of the powders were observed by a field emission scanning electron microscope (FE-SEM, JSM-6701F, JEOL Ltd.) with an acceleration voltage of 3 kV. The particle sizes of the TiO_2 powders were obtained from the SEM images.

2.6. Electrode preparation

Thick-film electrodes of TiO_2/MnO_2 composite were prepared by a gas-deposition (GD) method [10,11], which is also known as an aerosol deposition method [12,13]. This preparation method has a unique characteristic: GD process does not require any binder or conductive material. An aerosol consisting of metal oxide particles and a carrier gas is ejected through a nozzle, and is accelerated to high speeds of about 150–500 m s^{-1}. The oxide particles collide with a current collector substrate, generating a high impact energy to strongly stick the particles on the substrate. In addition, the particles adhere with each other by the intermixing at the interface. Consequently, the GD-film electrodes generally show a good mechanical durability and a decent electrical conductivity even though those do not contain binder and conductive material. In this study, the GD was performed under the following conditions: a nozzle diameter of 0.3 mm, a Ti current collector thickness of 20 μm, a He carrier gas differential pressure of 4.0×10^5 Pa, and a nozzle–substrate distance of 9 mm (Fig. S2). First, MnO_2 film was deposited on one surface of Ti substrate. Next, TiO_2 film was deposited on the reverse side of the substrate. In this study, we call the electrode consisting MnO_2, TiO_2, and Ti substrate "composite electrode" in the sense that MnO_2 electrode and TiO_2 electrode were combined into single electrode. The deposition area was 3.0 cm^2. The deposition amount of TiO_2 and MnO_2 were 300–400 μg and 30–50 μg. Their film

thicknesses were typically 40 μm and 7 μm, respectively. A pseudocapacitive charge-discharge behavior based on Na^+-adsorption/desorption was confirmed for an electrode of MnO_2 alone as a conventional electrochemical capacitor electrode (Fig.S3).

2.7. Photoelectrochemical measurements

Photoelectrochemical measurements were conducted at room temperature by using a beaker-type three-electrode cell (HX-113, Hokuto Denko Co., Ltd.) and a control system including an electric circuit and an impedance analyzer (CompactStat.h 20250e, Ivium Technologies). Figure 2 illustrates a photoelectrochemical measurement system. This system has been basically fabricated in the previous study [8]. In the beaker cell, a titanium wire with a diameter of 0.5 mm and an Ag/AgCl electrode were used as the counter and reference electrodes, respectively. The electrolyte was a Na_2SO_4 aqueous solution with a concentration of 0.5 mol L^{-1}. A Xe lamp (SOLAX XC-100EFSS, SERIC Co., Ltd.) with a power density of about 1.0 kW m^{-2} was used as a solar simulator. The load resistance was 77 kΩ. In a photo-charge process, the TiO_2/MnO_2 electrode was irradiated for 30 s in open-circuit condition. A discharge process was subsequently performed for 20 s in short-circuit condition between the TiO_2/MnO_2 electrode and the Ti wire electrode. For a control experiment, the discharge current was measured after the electrodes were kept in open-circuit condition for 10 s without irradiation (a dark-charge process). The discharge capacity was defined as an integrated difference in the two kinds of discharge currents after the photo-charge process and dark-charge process at the first cycles.

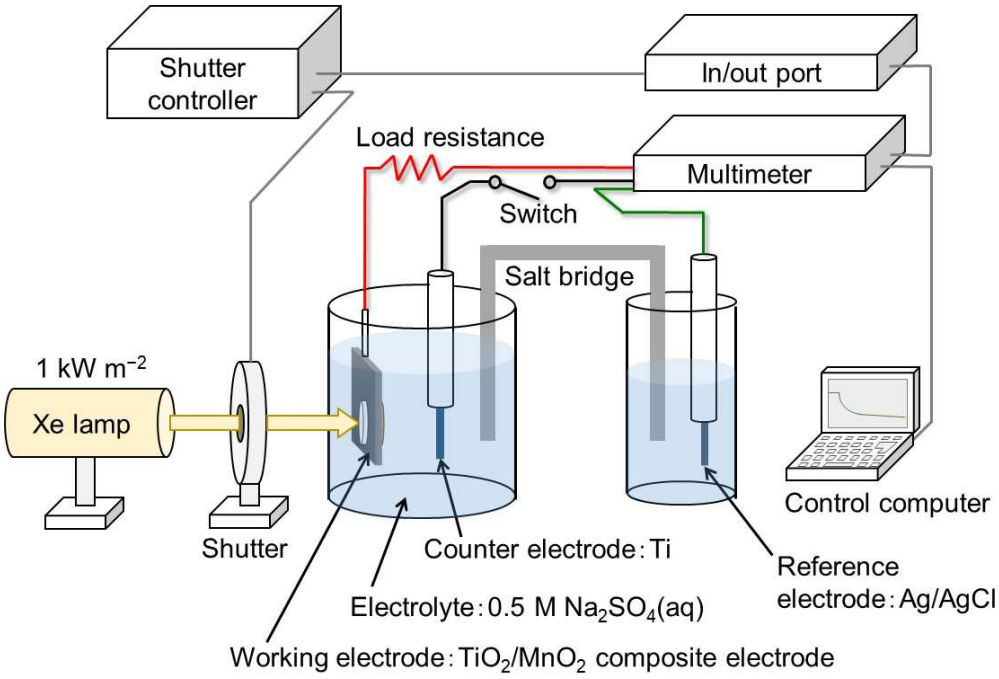

Figure 2. Schematic illustration of photo-charge and discharge measurement system for photoelectrochemical capacitor electrode.

3. Result and discussion

3.1. Crystal structure and morphology of TiO_2

Figure 3 shows XRD patterns of TiO_2 powders synthesized by a hydrothermal (HT) method and a sol–gel method. For comparison, the figure represents a commercial (com.) rutile TiO_2 also. In cases of HT synthesis and sol–gel synthesis, all diffraction peaks could be assigned as rutile TiO_2 phase (Inorganic Crystal Structure Database, ICSD No.00-021-1276). It was confirmed that single phase of rutile TiO_2 was obtained as we expected. The diffraction peaks of HT synthesis TiO_2 and commercial TiO_2 were sharper than those of sol–gel synthesis TiO_2. The crystalline sizes were estimated from full width half-maximum of the peaks by using the Scherrer equation. The crystallite sizes estimated of HT, commercial, and sol–gel TiO_2 were 31, 41, and 17 nm, respectively. These results demonstrated that HT TiO_2 has a good crystallinity comparable to that of commercial one.

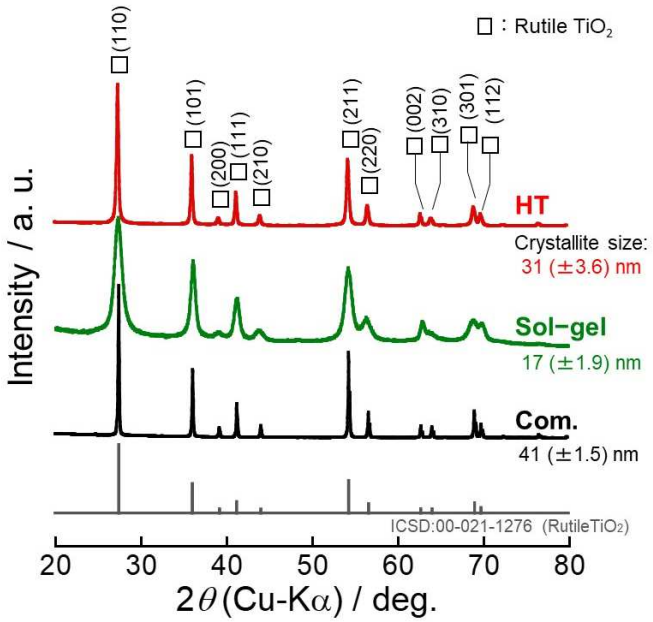

Figure 3. XRD patterns of TiO_2 particles prepared by hydrothermal (HT) method and sol-gel method, and commercial (com.) TiO_2.

Figure 4 displays SEM images of these TiO_2 particles. A nanorod morphology was observed for the HT TiO_2 particles. As the origin of the nanorod morphology, an Ostwald ripening mechanism is suggested: smaller TiO_2 particles are dissolved and are redeposited onto the growing rod structures during an autoclave synthesis [14]. The nanorod edges consist of {001} and {101} facets, whereas the nanorod side planes are comprised of {110} facets [15]. Since surface free energies of the {001} and {101} facets are much higher than those of the {110} facets, the crystal growth of rutile nanorod is preferentially enhanced in its *c*-axis directions [15]. The particle size of HT TiO_2 was estimated to be 63 nm. Note that not the length but the width of nanorod was defined as the particle size in this study because we will discuss an accessibility of photoexcited carriers from inside to surface of TiO_2 particles. On the other hand, spherical morphologies were fond for the sol−gel TiO_2 and commercial one. Their particle sizes were 64 and 210 nm.

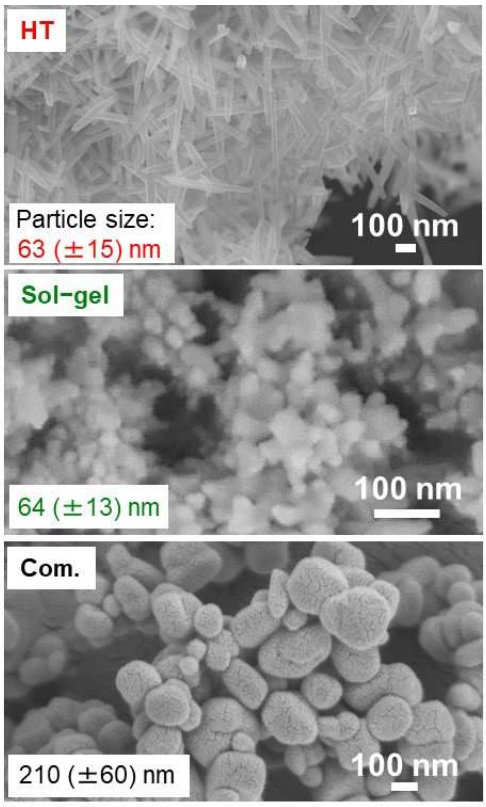

Figure 4. SEM images of TiO_2 particles prepared by hydrothermal (HT) method and sol-gel method, and commercial (com.) TiO_2.

3.2. Photovoltage of TiO_2 electrodes.

Figure 5(a) shows potential variations of TiO_2 electrodes during light irradiation. The electrodes are denoted as TiO_2(HT), TiO_2(sol−gel), and TiO_2(Com.) in the figure. The TiO_2(Com.) electrode showed a potential drop in the initial 10 s, and subsequently maintained the constant potential. This indicates that electrons accumulated in the electrode during the initial 10 s, and that there was subsequently an equilibrium between the electron generation and the recombination of electron−hole pairs. In case of TiO_2(sol−gel), the electrode potential was gradually decrease for 30 s, suggesting a lower rate of the electron accumulation. In contrast, the TiO_2(HT) exhibited a steep potential drop in the initial 10 s, demonstrating an efficient electron accumulation. This reason is probably the better crystallinity of TiO_2 particles: the crystallite size of 31 nm for TiO_2(HT) is larger than that of 17 nm for TiO_2(sol−gel). The better crystallinity could suppress the recombination of electron−hole pairs because of a lower lattice defect density in the particles. In this study, the potential drop for 30 s was defined as the photovoltage. The TiO_2(HT) electrode showed higher photovoltage of 206 mV, whereas those of TiO_2(sol−gel) and TiO_2(Com.) electrodes were 149 mV and 117 mV.

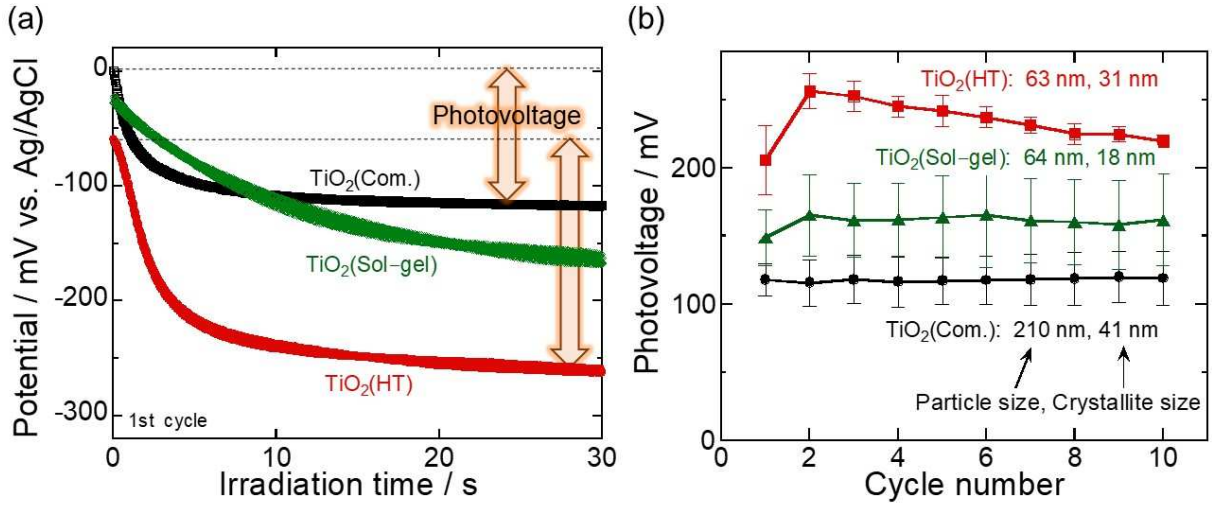

Figure 5. (a) Potential variation of various TiO_2 electrodes during light irradiation. (b) Photovoltages of electrodes consisted of TiO_2 with different particle sizes and crystallite sizes.

Figure 5(b) compares dependences of the photovoltages on charge–discharge cycle numbers. Values in the parentheses represent the particle size and the crystallite size obtained by the SEM observation and the XRD analysis. A constant photovoltage of 117 mV was observed for TiO_2(Com.) electrode. The TiO_2(sol–gel) showed 1.4 times higher photovoltages compared to TiO_2(Com.). The reason is probably that there is a larger contact area between electrode surface and electrolyte because the electrode was prepared by using TiO_2 with smaller particle size, which is more preferable for the effective hole consumption and the resulting efficient electron accumulation. The TiO_2(HT) electrode attained the further enhancement: the photovoltage of 256 mV was achieved at the second cycle, which is 2.2 times higher than that of TiO_2(Com.) electrode. The enhanced photovoltage possibly originates not only from the smaller particle size but also from the higher crystallinity of TiO_2. It is suggested that the electron–hole recombination was suppressed in TiO_2 synthesized by HT method because it has a lower density of lattice defect

trapping the photoexcited carriers. We focus hereafter TiO_2(HT) showing the highest photovoltage because it is suitable for enhancing a photoelectrochemical capacitor property of a TiO_2/MnO_2 composite electrode.

We have confirmed that the electrode of TiO_2 alone showed a very small discharge capacity less than 0.1 mA h g^{-1}. MnO_2 polymorphs have various tunnels in their crystal structures [16,17], which are very suitable for Na^+ storage as electrode materials of electrochemical supercapacitor. Thus, the authors chose an electrode material adsorbing Na^+ in a composite electrode [8]. Figure 6 shows the discharge currents measured for composite electrodes consisted of TiO_2(Com.)/MnO_2 and TiO_2(HT)/MnO_2. This figure plots two kinds of discharge currents: a current after photo-charge process $I_{photo}(t)$ and one after dark-charge process $I_{dark}(t)$. A rapid decay of the discharge current after the photo-charge was observed for the TiO_2(Com.)/MnO_2 composite electrode. By contrast, the TiO_2(HT)/MnO_2 electrode did not show the rapid decay, and maintained a constant discharge current of 400 μA cm^{-2} during the initial 3 s. This result indicates that the electron accumulation and the resulting Na^+ adsorption were more sufficient. Discharge capacities (Q) were calculated from areas enclosed by the two kinds of discharge currents, $I_{photo}(t)$ and $I_{dark}(t)$. The calculation equation can be described as follows:

$$Q = \int \{ I_{photo}(t) - I_{dark}(t) \} dt.$$

The TiO_2(Com.)/MnO_2 electrode delivered the discharge capacity of 1.4 mA h g^{-1}. On the other hand, the TiO_2(HT)/MnO_2 electrode exhibited 3.4 mA h g^{-1}, which is 2.4 times larger than that of TiO_2(Com.)/MnO_2. This improvement rate in the capacity approximately agrees to that in the photovoltage (2.2 times), which is a reasonable result. These results demonstrated that charge voltage and Na^+ adsorption amount for MnO_2 could be increased by changing from commercial TiO_2 to HT TiO_2 showing the doubled photovoltage. In this study, the improved photovoltage of TiO_2 could enhance the photoelectrochemical capacity property. On the other hand, the optimization of electrode materials is also expected to enhance the property. In the near future, we will develop new composite electrodes by using MnO_2's polymorphs [16,17] or Li_3VO_4 [18] as electrode materials with high capacities.

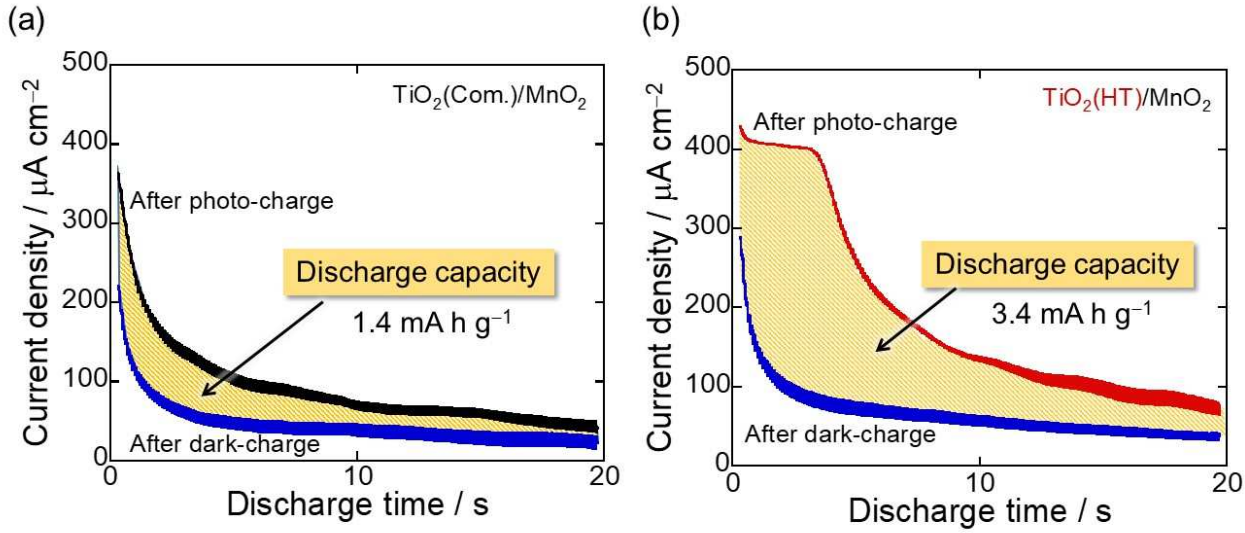

Figure 6. Changes in discharge currents of (a) TiO_2(Com.)/MnO_2 composite electrode and (b) TiO_2(HT)/MnO_2 composite electrode.

4. Conclusions

We prepared composite electrodes consisting of TiO_2 particles and MnO_2 particles by the GD method, and evaluated their photoelectrochemical capacitor properties by light irradiation for those in aqueous electrolytes. By employing different synthesis method of TiO_2 particles, we prepared TiO2 particles with different particle sizes and crystallite sizes. The hydrothermally-synthesized TiO_2 has the particle size of 63 nm, which is comparable to that of sol–gel synthesized one, whereas the particle size of commercial TiO_2 was as large as 240 nm. The crystallite size of the hydrothermally-synthesized TiO_2 was larger than that of the sol–gel synthesized one. An electrode of sol–gel TiO_2 showed 1.4 times higher photovoltages compared with an electrode of commercial TiO_2. This probably originates from a larger contact area between electrode surface and electrolyte because of its smaller particle size. The large contact area is preferable for an effective hole consumption and the resulting efficient electron accumulation. A further enhancement was

attained for an electrode of the hydrothermally-synthesized TiO_2: it showed a 2.2 times higher photovoltage than that of the electrode of commercial TiO_2. This enhancement in photovoltage could improve a photoelectrochemical capacitor property of TiO_2/MnO_2 composite electrode: the discharge capacity was increased 2.2 times by changing from commercial TiO_2 to the hydrothermally-synthesized TiO_2.

Acknowledgements

This work was partially supported by Japan Society for the Promotion of Science (JSPS) KAKENHI (16K05954, 17K17888, 17H03128), and by Electric Technology Research Foundation of Chugoku. A part of this work was supported by the Japan Association for Chemical Innovation (JACI). The authors thank Mr. S. Ohnishi and Mr. T. Tamura for their helpful assistance of hydrothermal syntheses of TiO_2 and MnO_2. The author appreciates Mr. Y. Yoshida for the customization of electrical circuit.

References

[1] T. N. Murakami, N. Kawashima, T. Miyasaka, A high-voltage dye-sensitized photocapacitor of a three-electrode system, *Chem. Commun.*, (2005) 3346–3348.

[2] Y. Takahashi and T. Tatsuma, Visible light-induced photocatalysts with reductive energy storage abilities, *Electrochem. Commun.*, **10** (2008) 1404–1407.

[3] J. Juodkazytė, B. Šebeka, P. Kalinauskas, K. Juodkazis, Light energy accumulation using Ti/RuO_2 electrode as capacitor, *J. Solid State Electrochem.*, **14** (2010) 741–746.

[4] T. Chen, L. Qiu, Z. Yang, Z. Cai, J. Ren, H. Li, H. Lin, X. Sun, H. Peng, A wire-shaped device based on aligned carbon nanotube fibers wrapped around a TiO_2 nanowire, *Angew. Chem. Int. Ed.*, **51** (2012) 11977–11980.

[5] M. Skunik-Nuckowska, K. Grzejszczyk, P. J. Kulesza, L. Yang, N. Vlachopoulos, L. Häggman, E. Johansson, A. Hagfeldt, Integration of solid-state dye-sensitized solar cell with metal oxide charge storage material into photoelectrochemical capacitor, *J. Power Sources*, **234** (2013) 91–99. .

[6] R. Liu, Y. Liu, H. Zou, T. Song, B. Sun, Integrated solar capacitors for energy conversion and storage, *Nano Research*, **10** (2017) 1545−1559.

[7] H. Usui, O. Miyamoto, T. Nomiyama, Y. Horie, T. Miyazaki, Photo-rechargeability of TiO_2 film electrodes prepared by pulsed laser deposition, *Sol. Energy Mater. Sol. Cells*, **86** (2005) 123−134.

[8] H. Usui, K. Koseki, T. Tamura, Y. Domi, H. Sakaguchi, Light energy storage in TiO_2/MnO_2 composite electrode for photoelectrochemical capacitor, *Mater. Lett.*, **186** (2017) 338−340.

[9] H. Usui, S. Yoshioka, K. Wasada, M. Shimizu, H. Sakaguchi, Nb-Doped Rutile TiO_2: a Potential Anode Material for Na-Ion Battery, *ACS Appl. Mater. Interfaces*, **7** (2015) 6567−6573.

[10] H. Sakaguchi, T. Toda, Y. Nagao, T. Esaka, Anode Properties of Lithium Storage Alloy Electrodes Prepared by Gas-Deposition, *Electrochem. Solid-State Lett.*, **10** (2007) J146−J149.

[11] H. Usui, Y. Kiri, H. Sakaguchi, Effect of carrier gas on anode performance of Si thick-film electrodes prepared by gas-deposition method, *Thin Solid Films*, **520** (2012) 7006−7010.

[12] J. Akedo, Aerosol Deposition of Ceramic Thick Films at Room Temperature: Densification Mechanism of Ceramic Layers, *J. Am. Ceram. Soc.*, **89** (2006) 1834−1839.

[13] J. Akedo, Room temperature impact consolidation (RTIC) of fine ceramic powder by aerosol deposition method and applications to microdevices, *J. Thermal Spray Tech.*, **17** (2008) 181−184.

[14] A. Mamakhel, C. Tyrsted, E. D. Bøjesen, P. Hald, B. B. Iversen, Direct Formation of Crystalline Phase Pure Rutile TiO_2 Nanostructures by a Facile Hydrothermal Method, *Cryst. Growth Des.*, **13** (2013) 4730−4734.

[15] A. Wisnet, S. B. Betzler, R. V. Zucker, J. A. Dorman, P. Wagatha, S. Matich, E. Okunishi, L. Schmidt-Mende, C. Scheu, Model for Hydrothermal Growth of Rutile Wires and the Associated Development of Defect Structures, *Cryst. Growth Des.*, **14** (2014) 4658−4663.

[16] S. Devaraj and N. Munichandraiah, Effect of Crystallographic Structure of MnO_2 on Its Electrochemical Capacitance Properties, *J. Phys. Chem. C*, **112** (2008) 4406−4417.

[17] O. Ghodbane, J.-L. Pascal, F. Favier, Microstructural Effects on Charge-Storage Properties in MnO_2-Based Electrochemical Supercapacitors, *ACS Appl. Mater. Interface*, **1** (2009) 1130−1139.

[18] E. Iwama, N. Kawabata, N. Nishio, K. Kisu, J. Miyamoto, W. Naoi, P. Rozier, P. Simon, K. Naoi, Enhanced Electrochemical Performance of Ultracentrifugation-Derived nc-Li_3VO_4/MWCNT Composites for Hybrid Supercapacitors, *ACS Nano*, **10** (2016) 5398−5404.

Figure Captions

Figure 1. Photo-charge and discharge mechanisms of TiO_2 electrode for photoelectrochemical capacitor.

Figure 2. Schematic illustration of photo-charge and discharge measurement system for photoelectrochemical capacitor electrode.

Figure 3. XRD patterns of TiO_2 particles prepared by hydrothermal (HT) method and sol–gel method, and commercial (com.) TiO_2.

Figure 4. SEM images of TiO_2 particles prepared by hydrothermal (HT) method and sol–gel method, and commercial (com.) TiO_2.

Figure 5. (a) Potential variation of various TiO_2 electrodes during light irradiation. (b) Photovoltages of electrodes consisted of TiO_2 with different particle sizes and crystallite sizes.

Figure 6. Changes in discharge currents of (a) TiO_2(Com.)/MnO_2 composite electrode and (b) TiO_2(HT)/MnO_2 composite electrode.